Journal of Power Sources 195 (2010) 3485–3489

Contents lists available at ScienceDirect

Journal of Power Sources

journal homepage: www.elsevier.com/locate/jpowsour

Short communication

Characterization and voltammetric behavior of $Pt_yMo_zO_x$/C electrodes prepared by the thermal decomposition of polymeric precursors

Ana C.R. Aguiar, Paulo Olivi*

Departamento de Quimica, Faculdade de Filosofia, Ciências e Letras de Ribeirão Preto, Universidade de São Paulo, Av. Bandeirantes 3900, CEP 14040-901, Ribeirão Preto, SP, Brazil

ARTICLE INFO

Article history:
Received 16 November 2009
Accepted 10 December 2009
Available online 21 December 2009

Keywords:
Platinum
Molybdenum
Electrocatalyst
Fuel cell

ABSTRACT

Carbon-supported catalysts containing platinum and molybdenum oxide are prepared by thermal decomposition of polymeric precursors. The $Pt_yMo_zO_x$/C materials are characterized by energy dispersive X-ray spectroscopy, transmission electron microscopy, and X-ray diffraction. The catalysts present a well-controlled stoichiometry and nanometric particles. Molybdenum is present mainly as the MoO_3 orthorhombic structure, and no Pt alloys are detected. The voltammetric behavior of the electrodes is investigated; a correlation with literature results for PtMo/C catalysts prepared by other methods is established. The formation of soluble species and the aging effect are discussed.

1. Introduction

The interest in the development of energy conversion devices has increased in the last decades, and fuel cell technology has been considered a promising alternative for clean electric power generation with high efficiency [1,2]. Several cell types are currently being investigated, and one that has attracted the most interest is the proton exchange membrane fuel cell (PEMFC) [1]. Besides hydrogen, methanol has emerged as an attractive liquid fuel in this kind of device, since it is relatively cheap, easily stored and handled, and readily available; has a high energy density [3]; and can be used directly as a fuel in direct methanol fuel cells (DMFCs) [4].

Among the pure metals, platinum presents the best activity as anode material in these devices [5,6]. However, the presence of strongly adsorbed intermediates that block the electrode surface restricts its practical use [7]. Many modifications to Pt electrodes have been suggested, and the better results are associated with the introduction of a more oxidizable metal. Such metals generate oxygenated species in the vicinity of the Pt active sites at lower potentials, thereby enhancing CO oxidative desorption at these sites [8]. Among the elements used as co-catalysts in Pt electrodes are Ru [9], Sn [10], Mo [11], and W [12]. Molybdenum is known for its beneficial co-catalytic effect in CO oxidation, not to mention that it has been used for methanol [13], formic acid [14], and ethanol [15] oxidation. Nevertheless, the behavior of molybdenum is very complex since it may present several oxidation states and might form distinct soluble species and various oxides. This poses a great difficulty to understanding the electrocatalysis mechanisms related to molybdenum.

Earlier studies on PtMo electrodes [16,17] have shown that the cyclic voltammograms of these catalysts are complex. In most cases, only a tentative ascription of the peaks is possible, thereby allowing for a qualitative distinction between the reduction–oxidation responses of Pt and Mo only. From the comparison between the electrochemical responses of pure Mo and that of a PtMo alloy combined with an ex situ XPS study of the surface species of the PtMo alloy, it has been suggested that Mo is present in the oxidized form in the entire potential window, changing from Mo^{3+} to Mo^{6+} as the potential increases [17–19].

Besides electrode composition, the preparation method plays an important role in electroactivity since it determines surface morphology, crystalline structure, and surface composition. Catalysts containing Pt and Mo have been prepared by chemical routes [13,16,19,20], electrochemical co-deposition methods [21–24], and thermal methods [25]. However, the stability of this kind of catalysts is still controversial. While some studies report the occurrence of molybdenum dissolution after only a few cycles [11,16], other investigations have shown the presence of stable molybdenum species after several cycles at potentials between 0.0 and 1.2 V in 0.5 mol L^{-1} H_2SO_4 [20,26,27].

The thermal decomposition of polymeric precursors has already been used to prepare $Pt_yMo_zO_x$ and $Pt_yRu_wMo_zO_x$ thin films over Ti plates [25]. The obtained catalysts furnished promising results concerning methanol electrooxidation, compared with pure Pt and other binary and ternary catalysts. In this work, we have prepared electrodes containing Pt and Mo dispersed on carbon powder by

* Corresponding author. Tel.: +55 16 3602 3869; fax: +55 16 3602 4838.
E-mail address: olivip@ffclrp.usp.br (P. Olivi).

0378-7753/$ – see front matter © 2009 Elsevier B.V. All rights reserved.
doi:10.1016/j.jpowsour.2009.12.041

the thermal decomposition of polymeric precursors in order to investigate their electrochemical behavior.

2. Experimental

The polymeric precursor method, also known as the Pechini method [28], was used for the preparation of $Pt_yMo_zO_x$/C catalysts with $y = 0.9$, 0.7, or 0.6 and $z = 0.1$, 0.3, or 0.4. The Pt precursor solution was prepared by dissolution of H_2PtCl_6 (Acros) in a citric acid and ethylene glycol solution at 90 °C, so as to obtain a metal, citric acid, and ethylene glycol molar ratio of 1:4:16, respectively. The Mo precursor solution was prepared in a similar way, by employing $MoCl_5$ and a metal, citric acid, and ethylene glycol molar ratio of 1:4:32. The precursor solutions were mixed with carbon powder (Vulcan XC 72) in appropriate proportions, in order to achieve a 30% metal loading. The obtained mixtures were calcined at 400 °C in oxygen atmosphere, for 1 h. The prepared electrocatalyst powders (2 mg) were dispersed in water (0.45 mL) and Nafion® 5% solution (0.05 mL, FLUKA), and taken to the ultrasound for 120 min. This suspension (60 μL) was deposited on a gold disc with 0.2 cm^2 surface area, fixed on a glass tube.

The elemental composition of the prepared $Pt_yMo_zO_x$/C catalysts was verified by energy dispersive X-ray spectroscopy (EDX). This analysis was performed on a scanning digital microscope (SDM) 940 Zeiss-West Germany coupled to an X-ray Microanalysis Link Analytical QX 2000. The morphology of the electrocatalysts was investigated by transmission electron microscopy (TEM), accomplished on a JEOL/JEM-3010 Microscope, operating at 300 kV. The crystal structures of the electrocatalysts were examined by X-ray diffraction (XRD) in a Siemens D5005 diffractometer, employing a copper anode (radiation Cu Kα = 1.54056 nm).

The behavior of the electrodes was examined by cyclic voltammetry in H_2SO_4 0.5 mol L^{-1} solution, using a conventional three-electrode electrochemical glass cell. Platinized platinum was used as the counter electrode, and reversible hydrogen electrode (RHE) was the reference electrode. Analysis was performed using an EG&G Princeton Applied Research Potentiostatic/Galvanostatic, model 273A, coupled to a microcomputer.

3. Results and discussion

EDX global analyses of the catalysts were performed on different sample surfaces, and the results show that the atomic composition of the catalysts is close to the expected values, with a difference lower than 10%. Therefore, the methodology is efficient in maintaining the relationship between the different metals present in the electrode and to prevent component loss during calcination.

The TEM micrographs of the electrocatalysts (Fig. 1a) reveal the formation of small spherical particles dispersed on carbon, as well as particle clusters. The existence of clusters in these cases is undesirable because a major cause of catalytic activity loss in electrocatalysis is known to be due to particle aggregation [29,30]. Hence, this clustering leads to loss of active area. By analyzing particle size distribution histograms (Fig. 1b), it can be seen that the electrocatalysts present particle sizes lying between 1 and 30 nm, and most of these particles have size between 2 and 6 nm.

Fig. 2 presents the results of XRD for the powder containing catalysts dispersed on carbon at nominal compositions Pt/C, $Pt_{0.9}Mo_{0.1}O_x$/C, $Pt_{0.7}Mo_{0.3}O_x$/C, and $Pt_{0.6}Mo_{0.4}O_x$/C. A Mo/C powder was prepared for comparison purposes, and this material displays a MoO_3 orthorhombic structure (JCPDS 47-1320), whereas the Pt/C catalyst exhibits peaks due to the Pt FCC structure (JCPDS 65-2868).

The binary catalysts display also the peaks related to the Pt FCC structure, but the peak intensity of the Mo oxide phase is very small. Only in electrocatalysts containing a higher amount of molybde-

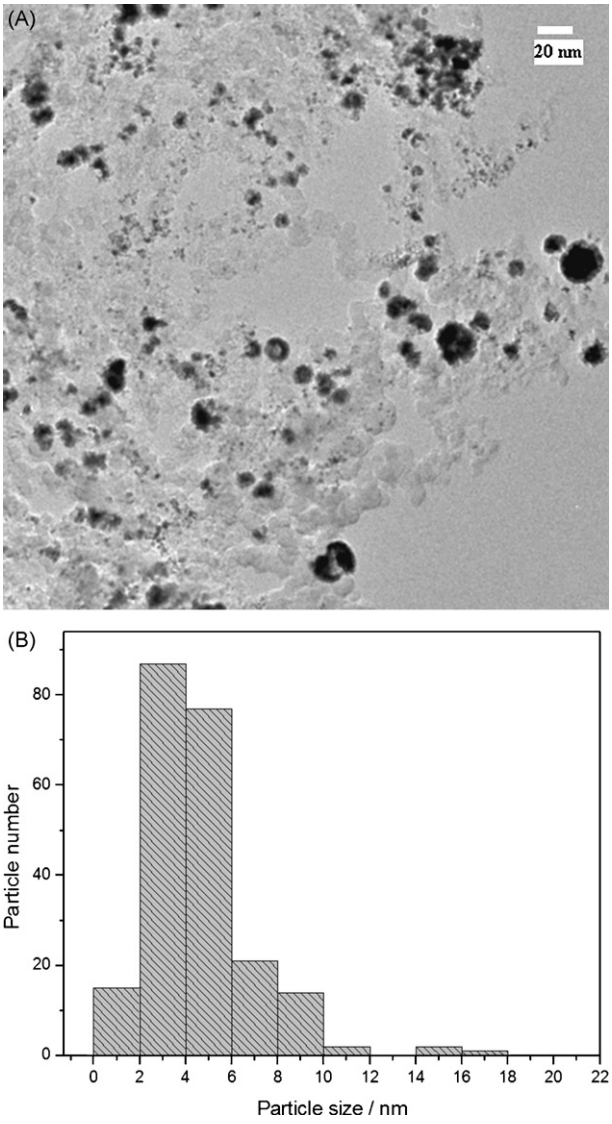

Fig. 1. TEM image (a) and Particles size distribution histogram (b) of $Pt_{0.7}Mo_{0.3}O_x$/C electrocatalyst.

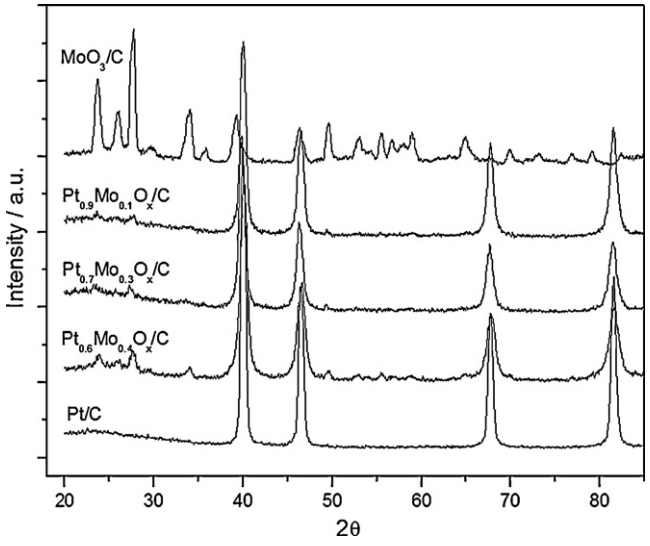

Fig. 2. XRD diffraction patterns of $Pt_yMo_zO_x$/C electrocatalysts.

num in the nominal composition ($Pt_{0.6}Mo_{0.4}O_x/C$) was it possible to clearly identify the presence of MoO_3. Furthermore, there are no significant displacements of the platinum peaks in any of the diffractograms obtained for the analyzed catalysts, showing that formation of alloys in these electrocatalysts does not occur.

Fig. 3a shows a typical cyclic voltammogram of Pt/C and $Pt_yMo_zO_x/C$ binary electrodes. The voltammogram of the Pt/C catalyst agrees with the behavior expected for pure Pt electrodes. For the $Pt_{0.6}Mo_{0.4}O_x/C$ electrode, two regions present well defined peaks due to the presence of Mo species: the positive potential scan reveals one peak at 0.32 V/RHE and several peaks between 0.52 and 0.67 V/RHE. The presence of these two regions suggests that Mo oxidation involves different oxidation states. The first peak at ca. 0.32 V can be attributed to the oxidation of MoO_2 to MoO_3, which is in accordance with the thermodynamic potential for the following reaction [31,32]:

$$MoO_2 + H_2O \leftrightarrows MoO_3 + 2H^+ + 2e^- \quad (1)$$

The existence of MoO_2 in the surface was not expected since it had not been detected by XRD. However, the cyclic voltammetry experiments were initiated at 0.05 V, which is sufficient to reduce MoO_3 to MoO_2. This behavior is clearly identified at the beginning of the voltammogram, where a high cathodic current is observed. The continuous potential cycling (Fig. 3b) gives evidence of a steady decrease in the peak at 0.32 V/RHE, which can be attributed to formation of Mo soluble species in acid solution. Irreversible Mo loss from the electrode surface has been previously reported in the literature [14,15,33]. The MoO_3 oxide is soluble in acid solutions [34], resulting in the formation of $HMoO_4^-$ species, the most stable soluble species in the pH value of the electrolyte solution [31]:

$$MoO_3 + H_2O \leftrightarrows HMoO_4^- + H^+ \quad (2)$$

In Fig. 3a, a cathodic peak at 0.16 V is also observed. When the electrode is submitted to continuous cycling (Fig. 3b), this cathodic peak also decreases and must be associated with MoO_3 reduction, leading to formation of MoO_2 oxide. The continuous solubilization of MoO_3 results in reduction of both anodic and cathodic peaks.

In order to confirm the nature of the observed dissolution, an experiment was carried out to determine the effect of the aging of the suspension used in the preparation of the working electrodes. The suspension prepared with the $Pt_{0.9}Mo_{0.1}O_x/C$ powder in a nafion/water solution, as described in the experimental section, was used in the preparation of electrodes after being left to stand for 0, 3, and 6 days. The voltammetric behavior of the resulting electrodes was evaluated between 0.05 and 0.9 V in 0.5 mol L^{-1} H_2SO_4 solution at a 50 mV s^{-1} scan rate, and Fig. 3c depicts the first cyclic voltammograms of the electrodes prepared in these conditions. This figure clearly shows that the MoO_3/MoO_2 transition peaks at 0.32 and 0.16 V decrease when the electrodes prepared with the fresh suspension and the electrodes prepared with the

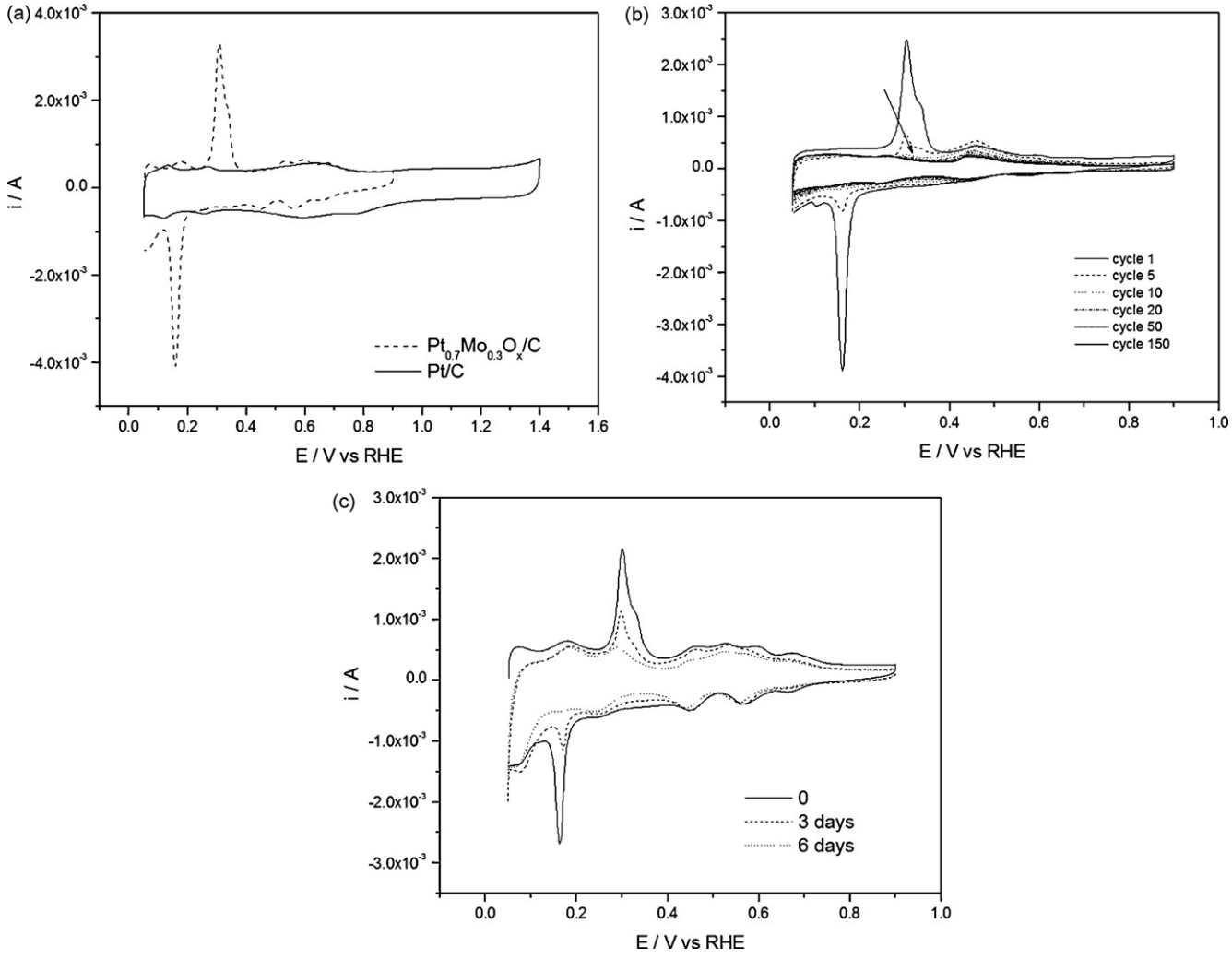

Fig. 3. Cyclic voltammograms of (a) Pt/C and $Pt_{0.6}Mo_{0.4}O_x/C$ in 0.5 mol L^{-1} H_2SO_4, (b) $Pt_{0.9}Mo_{0.1}O_x/C$, 150 cycles in 0.5 mol L^{-1} H_2SO_4 and (c) $Pt_{0.9}Mo_{0.1}O_x/C$ in 0.5 mol L^{-1} H_2SO_4 prepared with fresh suspension and with aged suspension.

suspension aged for 3 and 6 days are compared. This behavior confirms that MoO_3 is dissolved in the electrode surface, and that this species is related with the peak at 0.32 V.

Some peaks in the region between 0.52 and 0.67 V/RHE are also observed in the voltammograms of Fig. 3. Lebedeva and Janssen [16] have found similar results using PtMo/C bimetallic anodes and they attributed these peaks to the existence of non-alloyed Mo, which can undergo an oxidation reaction in this potential range. However, a clear ascription of the peaks has not yet been presented.

The results in Fig. 3 show that the peaks in the 0.52/0.67 V potential range do not disappear after reduction in the peak at 0.32 V. This indicates that they are related to the oxidation of distinct species, and that they are not related to sequential reaction steps.

A series of Mo-oxide structures with Mo_nO_{3n-1} stoichiometries, like Mo_8O_{23}, Mo_4O_{11}, and Mo_3O_8, are feasible between MoO_3 and the MoO_2 distorted rutile structures [35]. These oxides present non-stoichiometric Mo:O ratios and mixed valences between Mo^{5+} and Mo^{6+}. In the XRD results, the only detected Mo oxide species was MoO_3, which presents the highest molybdenum oxidation state. However, the presence of other oxide structures at the catalyst surface cannot be discarded on the basis of the XRD data since they can be present in small quantities and have low crystallinity. XPS data obtained for $PtMoO_x$ prepared by several methods showed the presence of Mo in the +4, +5, and +6 valences [32,36]. The Mo_nO_{3n-1} oxides are less soluble than MoO_3, and the transition from Mo^{5+} to Mo^{6+} may occur in a more positive potential than that expected for the MoO_2 to MoO_3 transition. The existence of a series of peaks in the 0.52/0.67 V range are thus attributed to oxidation/reduction of the Mo present in the Mo_nO_{3n-1} structures.

Complementary voltammetric studies were carried out, in order to verify the electrochemical behavior of the solubilized species. For this purpose, a couple of $Pt_{0.9}Mo_{0.1}O_x$/C electrodes were submitted to 150 voltammetric cycles in a 0.5 mol L^{-1} H_2SO_4 solution, to accumulate the species in solution. A smooth Pt electrode was then introduced into that solution, and a subsequent cyclic voltammetry experiment was carried out. The result is presented in Fig. 4.

The voltammograms in Fig. 4 display the peaks corresponding to the Mo soluble species oxidation/reduction reactions at 0.44 and 0.42, respectively [31]. The obtained cyclic voltammograms are similar to the voltammograms obtained in Na_2MoO_4 solutions [21,22,32,36] and must correspond to the following reaction:

$$MoO_2 + 2H_2O \leftrightarrows HMoO_4^- + 3H^+ + 2e^- \quad (3)$$

By comparing the above data with the results presented in the literature, it is possible to identify several similar aspects in the voltammetric behavior of Mo species, despite the difference in the employed preparation methods. Many authors [14,22,32,36–38] have prepared PtMo electrodes by electrodeposition in Na_2MoO_4 solution. This process corresponds to reaction (3) above, and the voltammetric behavior is similar to that observed in Fig. 4, where the solubilized species were deposited on a smooth Pt electrode. Dos Anjos et al. [15] have prepared PtMo bimetallic electrodes by arc-melting furnace process. These authors also observed the peak at ca. 0.45 V, which was attributed to the solubilization of non-alloyed Mo. Martínez-Huerta et al. [19] have prepared different $PtRu/MoO_x$/C catalysts by the deposition–precipitation method, using $MoCl_5$ and also MoO_3 from Aldrich. For the samples prepared with $MoCl_5$, these authors observed a peak at 0.44 V in the positive potential scan and a peak at 0.40 V in the negative scan. These peaks were attributed to the Mo^{5+}/Mo^{6+} transition to form MoO_x ($2.5 < x < 3$). However, this transition is expected to occur at potentials higher than 0.54 V [26], so the peak at 0.44 V is probably also related to the process described in reaction (3). The electrode prepared by Martínez-Huerta et al. [19] with MoO_3 from Aldrich presented the same peak at 0.44 V and another anodic peak at ca. 0.27 V. These authors observed a decrease in the peak at 0.27 V after 50 cycles, due to formation of Mo soluble species.

Lebedeva and Janssen [16] prepared PtMo/C catalysts by a chemical method employing formaldehyde or formic acid as reducing agent in $MoCl_5$ solutions. The voltammograms obtained in 0.5 mol L^{-1} H_2SO_4 solutions are similar to the voltammograms in Fig. 3 after the peak at 0.32 V is completely diminished. In both cases, anodic peaks between 0.52 and 0.67 V are observed. Lebedeva and Janssen [16] attributed this process to the presence of non-alloyed Mo, but these authors did not ascribe it to a specific reaction. On the other hand, Mukerjee and Urian [26] analyzed the behavior of PtMo from ETEK by XAS in situ and found that the Mo^{5+}/Mo^{6+} transition occurs at potentials higher than 0.54 V. The possible oxides that present Mo in the +5 and +6 states can be represented by Mo_nO_{3n-1} as discussed above. Since at least three peaks can be identified in Fig. 3 in the 0.52/0.67 V potential range, they can be related to the presence of several non-stoichiometric Mo oxides.

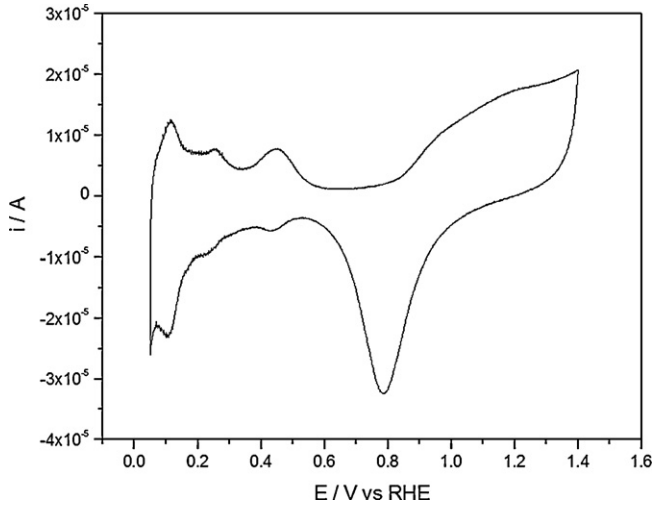

Fig. 4. Cyclic voltammograms of smooth Pt, in 0.5 mol L^{-1} H_2SO_4 + Mo dissolved species.

4. Conclusion

The synthesis of the carbon-supported $Pt_yMo_zO_x$ electrocatalysts via thermal decomposition of polymeric precursors is efficient in maintaining the ratio between the different metals and to prevent component loss during calcination. The catalysts must be composed basically by metallic Pt and MoO_3, since those were the only identified phases. No evidence of PtMo alloy formation was found. The electrochemical behavior of the obtained materials was investigated by cyclic voltammetry in sulfuric acid solutions. It was verified that the MoO_3 initially present in the electrode surface could be slowly solubilized, to form MoO_4^{2-} species. MoO_3 could be also reduced to MoO_2 during the negative scan. Three different anodic peaks between 0.52 and 0.67 V were detected and attributed to the Mo^{5+}/Mo^{6+} transition present in non-stoichiometric molybdenum phases.

The aging of the catalysts in aqueous solutions showed that MoO_3 dissolution leads to distinct voltammetric behavior depending on the aging period. A correlation between the voltammetric behavior and the results presented in the literature for PtMo catalysts prepared by other methods was established.

Acknowledgements

The authors thank Conselho Nacional de Desenvolvimento Científico e Tecnológico (CNPq), Financiadora de Estudos e Projetos

(FINEP), and Fundação Coordenação de Aperfeiçoamento de Pessoal de Nível Superior (CAPES) for financial support.

References

[1] E.V. Spinacé, A. Oliveira Neto, E.G. Franco, M. Linardi, Quim. Nova 27 (4) (2004) 648–654.
[2] H. Wendt, M. Gotz, M. Linardi, Quim. Nova 4 (2000) 538–546.
[3] L.K. Verma, J. Power Sources 86 (2000) 464–468.
[4] T. Iwasita, Electrochim. Acta 47 (2002) 3663–3674.
[5] W. Vielstich, J. Braz. Chem. Soc. 14 (2003) 503–509.
[6] N. Markovic, H.A. Gasteiger, P.N. Ross, I. Villegas, M.J. Weaver, Electrochim. Acta 40 (1995) 91–98.
[7] L.P.R. Profeti, F. Hahn, K.B. Kokoh, P. Olivi, Can. J. Chem. 85 (2007) 923–929.
[8] A. Oliveira Neto, M.J. Giz, J. Perez, E.A. Ticianelli, E.R. Gonzalez, J. Electrochem. Soc. 149 (2002) A272–A279.
[9] Y.C. Wei, C.W. Liu, K.W. Wang, ChemPhysChem 10 (2009) 1230–1237.
[10] M. Götz, H. Wendt, Electrochim. Acta 43 (24) (1998) 3637–3644.
[11] A.A. Mikhailova, A.A. Pasynskii, Z.V. Dobrokhotova, V.A. Grinberg, O.A. Khazova, Russ. J. Electrochem. 44 (3) (2008) 303–312.
[12] L.X. Yang, C. Bock, B. MacDougall, J. Park, J. Appl. Electrochem. 34 (2004) 427–438.
[13] A. Oliveira Neto, J. Perez, W.T. Napporn, E.A. Ticianelli, E.R. Gonzalez, J. Braz. Chem. Soc. 11 (1) (2000) 39–43.
[14] C. Song, M. Khanfar, P.G. Pickup, J. Appl. Electrochem. 36 (2006) 339–345.
[15] D.M. Dos Anjos, K.B. Kokoh, J.M. LéGer, A.R. De Andrade, P. Olivi, G. Tremiliosi-Filho, J. Appl. Electrochem. 36 (2006) 1391–1397.
[16] N.P. Lebedeva, G.J.M. Janssen, Electrochim. Acta 51 (2005) 29–40.
[17] B.N. Grgur, N.M. Markovic, P.N. Ross, J. Phys. Chem. B 102 (1998) 2494–2501.
[18] B.N. Grgur, G. Zhuang, N.M. Markovic, P.N. Ross, J. Phys. Chem. B 101 (1997) 3910–3913.
[19] M.V. Martínez-Huerta, J.L. Rodríguez, N. Tsiouvaras, M.A. Peña, J.L.G. Fierro, E. Pastor, Chem. Mater. 20 (2008) 4249–4259.
[20] L.C. Ordóñez, P. Roquero, P.J. Sebastian, J. Ramírez, Catal. Today 107–108 (2005) 46–52.
[21] G. Samjeské, H. Wang, T. Löffler, H. Baltruschat, Electrochim. Acta 47 (2002) 3681–3692.
[22] T. Huang, J. Zhuang, A. Yu, J. Appl. Electrochem. 39 (2009) 1053–1058.
[23] Y. Márquez-Navarro, L. Galicia, V.H. Lara, G.D. Angel, J. Mex. Chem. Soc. 52 (1) (2008) 67–73.
[24] S.L. Gojkovic, A.V. Tripkovic, R.M. Stevanovic, N.V. Krstajic, Langmuir 23 (2007) 12760–12764.
[25] M.B. Oliveira, L.P.R. Profeti, P. Olivi, Electrochem. Commun. 7 (2005) 703–709.
[26] S. Mukerjee, R.C. Urian, Electrochim. Acta 47 (2002) 3219–3231.
[27] P. Roquero, L.C. Ordóñez, O. Herrera, O. Ugalde, J. Ramírez, Int. J. Chem. React. Eng. 5 (A99) (2007) 1–9.
[28] M.P. Pechini, U.S. Patent 3,330,697, 11 July 1967.
[29] T. Iwasita, H. Hoster, A. John-Anacker, W.F. Lin, W. Vielstich, Langmuir 16 (2000) 522–529.
[30] E. Antonili, J. Mater. Sci. 38 (2003) 2995–3005.
[31] M. Pourbaix, Atlas of Electrochemical Equilibrium in Aqueous Solution, Pergamon Press, NY, 1966.
[32] Y. Wang, E.R. Fachini, G. Cruz, Y. Zhu, Y. Ishikawa, J.A. Colucci, C.R. Cabrera, J. Electrochem. Soc. 148 (3) (2001) C222–C226.
[33] J.M. Jaksic, Lj. Vracar, S.G. Neophytides, S. Zafeiratos, G. Papakonstantinou, N.V. Krstajic, M.M. Jaksic, Surf. Sci. 598 (2005) 156–173.
[34] D.R. Lide, CRC Handbook of Chemistry and Physics, 89th edition, CRC Press, London, 2008/2009.
[35] N.N. Greenwood, W.A. Earnshaw, Chemistry of the Elements, 2ª edition, Elsevier, NY, 1997.
[36] H. Zhang, Y. Wang, E.R. Fachini, C.R. Cabrera, Electrochem. Solid-State Lett. 2 (9) (1999) 437–439.
[37] H. Nakajima, H. Kita, Electrochim. Acta 35 (5) (1990) 849–853.
[38] J. Lu, W.S. Li, J.H. Du, J.M Fu, J. New Mater. Electrochem. Syst. 8 (2005) 5–14.